PCCP

Accepted Manuscript

This is an *Accepted Manuscript*, which has been through the Royal Society of Chemistry peer review process and has been accepted for publication.

Accepted Manuscripts are published online shortly after acceptance, before technical editing, formatting and proof reading. Using this free service, authors can make their results available to the community, in citable form, before we publish the edited article. We will replace this *Accepted Manuscript* with the edited and formatted *Advance Article* as soon as it is available.

You can find more information about *Accepted Manuscripts* in the Information for Authors.

Please note that technical editing may introduce minor changes to the text and/or graphics, which may alter content. The journal's standard Terms & Conditions and the Ethical guidelines still apply. In no event shall the Royal Society of Chemistry be held responsible for any errors or omissions in this *Accepted Manuscript* or any consequences arising from the use of any information it contains.

ROYAL SOCIETY OF CHEMISTRY

www.rsc.org/pccp

Interaction between Calf Thymus DNA and Cationic Bottle-Brush Copolymers: Equilibrium and Stopped-Flow Kinetic Studies

Debabrata Dey,[†] Chiranjit Maiti,[†] Souvik Maiti,[‡] Dibakar Dhara*[†]

[†]*Department of Chemistry, Indian Institute of Technology Kharagpur, West Bengal 721302, India*

[‡]*Proteomics and Structural Biology Unit, Institute of Genomics and Integrative Biology, CSIR, Mall Road, Delhi 110007, India*

*Corresponding Author
Email: dibakar@chem.iitkgp.ernet.in, dibakar@live.in
Ph no: +91-3222-282326; Fax: +91-3222-282252

ABSTRACT: Interaction studies between a set of poly(ethylene glycol) (PEG) based cationic bottle-brush block copolymers (BBCPs) and calf-thymus DNA (*ct*DNA) were carried out using steady state fluorescence spectroscopy, UV melting and dynamic light scattering measurements. Results suggested that these cationic block copolymers could effectively bind with negatively charged DNA. Although electrostatic interaction is believed to be the predominant contributing factor in the overall binding process, hydrophobic interactions between the PEG chains and the DNA base pairs affected the binding process to some extent. Cationic block copolymers with higher PEG content were found to bind more efficiently with DNA. DLS studies revealed the details of the compaction process of elongated DNA chains into globular structure in presence of cationic block copolymers. Further, the kinetics of the DNA-cationic BBCP binding process was monitored via stopped-flow fluorescence technique. A general, a two-step mechanistic pathway was observed in case of all the cationic BBCP-DNA binding process and the relative rate constants ($k_1^{'}$ and $k_2^{'}$) were found to increase with the copolymer concentration. The first step corresponded to a fast electrostatic binding between the cationic BBCP and the anionic *ct*DNA, while the slow second step indicated a conformational change of the DNA polyplex that led to DNA compaction. In addition to the polymer-DNA charge ratios, the PEG content in the cationic BBCPs was found to have a significant effect on the kinetics of the *ct*DNA-BBCP polyplex formation.

KEY WORDS: polyelectrolytes, electrostatic interaction, hydrophobic interaction, fluorescence nucleic acid-polymer interactions, gene delivery agents.

INTRODUCTION:

In recent years, interactions of DNA with different cationic agents (e.g., multivalent cations, surfactants, polymers) have gained tremendous research interest, particularly owing to a rising interest in the field of non-viral gene delivery and gene transfection.[1-5] Although the DNA-cationic agent complexes offer the advantages of non-viral agents unlike their viral counterparts, they suffer from serious limitations like toxicity and lower solubility in aqueous medium.[6] DNA is a polyelectrolyte with high negative charge at physiological pH, owing to the presence of phosphate groups and has a structure that results from the various electrostatic and hydrophobic interactions between the different residues in the polynucleotide chain.[7] One serious limitation of gene delivery is the difficulty of transporting a DNA into a cell via the cell membrane, since it is repelled by the negatively charged cell membrane. However, on conjugation with a cationic agent that neutralizes the negative charge, DNA-based complexes are formed that possess some positive surface charge due to the presence of the cationic agent. This enables an easy approach of the complexed DNA towards the negatively charged cell membrane.[8] Moreover, complexation with cationic agents result in significant compaction of the native DNA, thus facilitating the internalization of the complexes into the cells.[7] In literature, it has been reported that factors like, the structures of the DNA-cationic complexes and their solubilities in the cell medium, also play important roles in determining their efficiencies as gene delivery agents.[6] Among the cationic agents, polymers provide some specific advantages, that has resulted in a shifted focus towards cationic copolymers as complexing agents with negatively charged DNA. The properties and architectures of the copolymers can be precisely controlled by employing living polymerization techniques for synthesizing them. Additionally, introduction of hydrophilic components like

polyethylene glycol and dextran into the copolymer structures improves the solubility and stability of the polyplexes while increasing the cell-survival and bio-distribution remarkably.[9-11]

It is well understood that the designing of cationic polymers with proper architectures is an extremely important aspect in polymeric gene delivery systems. In this context, block copolymers are very useful as they have the properties of each of the constituent homopolymers as well as a unique set of properties owing to the overall polymer structure. The necessary hydrophilic-hydrophobic balance and charge density can be achieved more precisely in case of a block copolymer due to the feasibility of controlling the length of the monomer sequences of either of the blocks via controlled polymerization.[12] Bottle-brush block copolymer is one of the several types block copolymers that have been synthesized using controlled polymerization techniques.

In a previous work, we have studied the interaction of DNA with cationic block copolymers having PEG in the backbone.[13] In the present study, we have used cationic bottle-brush block copolymers (BBCPs) containing hanging PEG chains (bristles of the bottle-brush), for interactions with DNA. These BBCPs have been synthesized earlier by RAFT polymerization[14-15] using [3-(methacryloylamino propyl)]trimethylammonium chloride (MAPTAC) and poly(ethylene glycol) methyl ether acrylate (PEGMA, M_n=480) as comonomers.[16] The length of the PEGMA was varied in the block copolymers, while the length of the cationic segment was kept unchanged. In order to make a comparative study, we have used the results from our earlier work on cationic homopolymer of MAPTAC to *ct*DNA interactions.[13,16] The structural changes occurring in DNA in presence of surfactants have been extensively studied by Lindman et al.[17-21] and Marchetti et al.,[8, 22] while Kabanov et al.[23-27] have explored the interactions between cationic block copolymers and DNA. In this work, we have investigated the possible structural and

conformational changes of DNA while interacting with the cationically charged BBCPs. Physicochemical tools like steady-state fluorescence spectroscopy, UV melting studies, dynamic light scattering studies and circular dichroism spectroscopy were used to get the necessary informations about structural changes occurring in Calf-thymus DNA (*ct*DNA).

Additionally, we have carried out a kinetic study of the copolymer-*ct*DNA complexation process. The life-time of the polyplexes and their dissociation *in vivo* plays vital role in determining their efficiency as a non-viral gene delivery agent. In this regard, the kinetics of DNA condensation also plays a very important role in gene transport. Techniques like stopped-flow fluorescence,[28] circular dichroism,[29] and potentiometry[30] have been used to monitor the kinetics of different DNA-surfactant systems. Here, we have used stopped-flow fluorescence technique, in which the sample and reagent solutions were mixed rapidly and measurements made almost instantaneously after mixing.[31-32] Fluorescence spectroscopy has been used to monitor the stopped-flow kinetics due to its higher time resolution and inherent sensitivity to fast processes. The effect of the cationic BBCPs-*ct*DNA charge ratios as well as the PEG content of the cationic BBCPs on the kinetics of DNA complexation process have been investigated in this work.

MATERIALS AND METHODS

Materials: Sodium salt of calf thymus DNA, ethidium bromide (3,8-diamino-5-ethyl-6-phenylphenanthridium bromide, EB) were purchased from Sigma-Aldrich and used without further purification. Cationic BBCPs and PMAPTAC (homopolymer of MAPTAC) used in this study were synthesized as described in a previous report from our group.[16] All the experiments were carried out using 10 mM potassium phosphate buffer (pH=7.4) with deionized water from a Milli-Q system. All other chemicals used in this study were of AR grade purity and used as

received. The concentration of DNA solutions are given in molarity units in terms of negatively charged phosphate groups in the DNA helix.

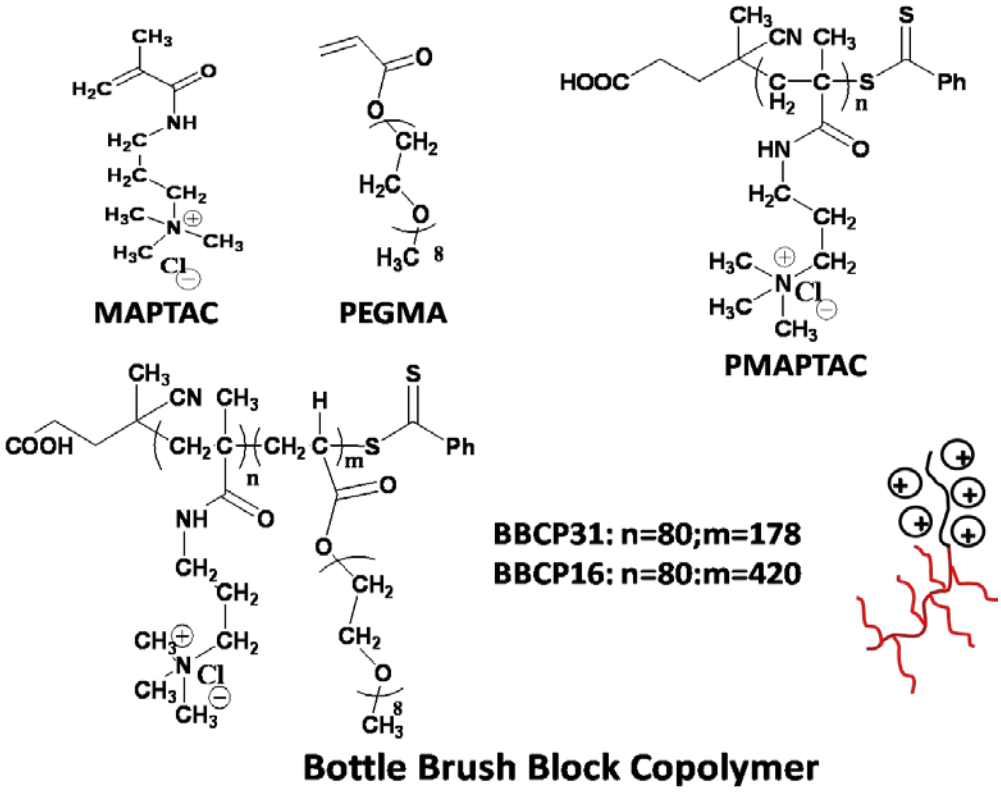

Scheme 1: Different components of the cationic bottle-brush copolymers (BBCPs) under the present study have been shown above. In the representative pictorial diagram of BBCPs (bottom right corner), the black line indicates cationic PMAPTAC units and red lines denote hanging PEGMA units from polymeric backbone.

Preparation of BBCP/DNA Complexes: The concentration of the DNA stock solution was measured by a Shimadzu UV-2450 UV spectrophotometer. The concentration of *ct*DNA (in terms of negatively charged phosphate group) was measured by its absorbance at 260 nm, the molar extinction coefficient (ε) being 6600 M^{-1} cm^{-1}. The concentration of DNA in terms of base pairs is exactly half the concentration of phosphate groups (ε = 13200 M^{-1} cm^{-1}). The ratio of

absorbance of DNA solution at 260 nm and 280 nm was found between 1.8 and 1.9. The absorbance at 320 nm was negligible, confirming the absence of any protein contamination. The stock solution of EB was prepared by dissolving 3.1 mg of EB in 2 ml of phosphate buffer. The concentration was determined by using UV-visible spectrophotometer (ε = 5600 M^{-1} cm^{-1} at 480 nm). EB solutions were stored in the dark at 4 °C before use. The BBCP stock solutions (5000 µM) were prepared by dissolving a known weight of each BBCP in a required volume of buffer solution. The BBCP-DNA polyplexes were prepared by mixing required amount of a polymer solution with a *ct*DNA solution in 10 mM potassium phosphate buffer solution (pH 7.4) to maintain an appropriate polymer-DNA charge ratio ($Z_{+/-}$). Next, the polyplex solutions were taken for vortexing and kept for equilibration for 2 h. The $Z_{+/-}$ ratio was expressed as the ratio of equivalents of cationic MAPTAC units to the number of negatively charged phosphate groups in DNA.

Steady State Fluorescence Spectroscopic Studies: Steady-state fluorescence emission spectra were collected using a Jobin Yvon Fluorolog spectrofluorometer. The excitation wavelength was set at 480 nm and the emission spectra were recorded in the wavelength range of 500 nm - 700 nm. The excitation slit and emission slit were kept fixed at 5 nm and 2 nm respectively. The DNA stock solutions and EB stock solutions were mixed (1 EB : 1 base pair) in the phosphate buffer and equilibrated for 10 min for preparing the DNA-EB complex. Required amounts of the BBCP stock solutions were added to a *ct*DNA - EB mixture (1 ml) in a quartz cuvette. After each single addition of BBCP solution, the resultant mixture was equilibrated for 10 min before recording the steady-state fluorescence spectrum. The working concentration of *ct*DNA in steady-state fluorescence spectroscopy was 25 µM in terms of negatively charged phosphate groups. The temperature was kept fixed at 25 °C in the experiment.

Measurement of the Melting Curve of BBCP-DNA Complexes: The thermal denaturation study was performed on Cary 100 UV-visible spectrophotometer equipped with a Peltier temperature controller. The recording chart reads temperature and absorbance differences between the reference and the sample cuvettes at 260 nm. All melting measurements were done at a fixed *ct*DNA concentration of 25 μM. Free *ct*DNA was dissolved in 10 mM phosphate buffer (pH 7.4). Different required volumes of BBCP solutions were separately mixed to a constant volume of *ct*DNA solution to obtain BBCP-*ct*DNA polyplexes of different charge ratios. The melting profiles of the DNA polyplexes were collected after 1 h of incubation of polyplex solutions at room temperature. The samples were heated from 40 °C to 95 °C at a scanning rate of 1.0 °C/min. Melting temperatures (T_m) were calculated from the melting curves.

Dynamic Light Scattering (DLS) Measurements: The average hydrodynamic size and the size distribution profiles of *ct*DNA and DNA-cationic BBCPs complexes were determined by dynamic light scattering measurements using a Malvern Nano ZS instrument employing a 4 mW He−Ne laser operating at a wavelength of 633 nm, scattering angle ~173° and an avalanche photodiode (APD) detector. The temperature was kept constant (25 °C) by circulating water through the cell holder using a JEIO TECH Thermostat (RW-0525GS). The concentration of *ct*DNA solution was same as in steady state fluorescence study. The addition of BBCP solutions continued from the charge ratio $Z_{+/-}$= 0 to $Z_{+/-}$= 12. A time interval of ~10 min was given to each DNA-BBCP mixture in order to attain equilibrium before recording the DLS data. CONTIN algorithm was used for deconvolution of the auto-correlation functions.

Circular Dichroism Measurements: CD spectra of native *ct*DNA and BBCP-*ct*DNA complexes at different charge ratios were recorded at pH~7.2 with a Jasco J-815 spectropolarimeter. The spectra were collected in the far-UV region (200-320 nm) with a quartz

cell with a path length of 10 mm was used. Three scans were accumulated at a scan speed of 50 nm per minute. Sample temperature was maintained at 25 °C using a Peltier thermostat. The buffer correction was made for every signal before recording the final data. The concentration of *ct*DNA was 100 μM (in terms of phosphate) in this study. The charge ratios were varied from 0 to 3.0.

Stopped-Flow Fluorescence Kinetic Studies: The kinetic measurements were done by using a SFA-20 rapid kinetics accessory (HI-Tech Scientific) in Jobin Yvon Fluorolog with a Peltier thermostat. The concentration of *ct*DNA - EB complex solution (EB : bp = 1.0) was 50 μM and three different concentration of the BBCP solutions were used i.e. 50, 150, 450 μM to achieve the charge ratios of the resultant DNA polyplex solutions as, $Z_{+/-}$= 1, 3, and 9 respectively, upon mixing of equal volume of two solutions. The excitation and emission monochromator were set at 480 nm and 590 nm respectively. At first, two separate syringes of the kinetic accessory were filled up with *ct*DNA - EB complex and BBCP solutions, respectively. Then equal volumes of both the solutions were injected at once into the sample chamber and this process was repeated for each run. The emission spectra of DNA-EB complex, in presence of BBCP, was monitored continuously, both before (t = 0 second) and after the injection. The dead time of the instrument was measured from the test reaction described elsewhere[33] and was found to be 5 ms for a 1:1 mixture. Control experiments were carried out by mixing a *ct*DNA - EB complex solution and buffer solutions without BBCPs. Possibility of photobleaching of the EB dye was ruled out since the fluorescence signal of *ct*DNA - EB complex remained unchanged during the course of the control experiment. The complex nature of the fluorescence decay curves indicated the possibility of presence of multiple steps and led us to assume a superposition of exponential terms to express the process:

$$I(t) = \sum A_i \exp(-t/\tau_i) \quad \text{(eq. 1)}$$

where I (t) is the fluorescence intensity at time t, A_i is the prefactor and τ_i is the pseudo-first order time constant. The reciprocal of time constant is the rate constant k_i of the reaction. The Nelder-Mead simplex method for minimizing eq. 1 was applied. The quality of the fits was assessed from the χ^2 value. Data analysis was performed using Origin 8.0 software.

RESULTS AND DISCUSSION

In the present work, the binding between the two synthesized BBCPs and the *ct*DNA were studied using EB dye exclusion assay (steady state fluorescence), melting experiments, DLS measurements and CD studies. For the sake of comparison, we have used cationic PMAPTAC homopolymer in all the experiment as a control, where the PEG content is nil. It helped us to monitor the effect of the hanging PEG units in the bottle-brush copolymers on their interactions with DNA. The compositions and the molecular weights of the polymers used in this study are given in Table 1.[16] We have used the molecular weight data determined from the ^{1}H NMR spectra of a polymer sample for calculation of the concentration of the polymer solution and the charge ratio, since it provides absolute and also more reliable number average molecular weight data for quantification. Kinetic study of the binding process between the BBCPs and *ct*DNA was done using stopped-flow fluorescence method. We believed that the kinetic study could impart some vital information and provide better understanding of the kinetic parameters of a stable DNA-polyplex formation process. We have earlier reported similar types of fast kinetic studies of DNA-polyplex formation with commercially available PAMAM dendrimers[34] and synthesized linear cationic block copolymers.[13]

Table 1: Composition, molecular weight, number of cationic units per polymer chain in the synthesized cationic block copolymers.[16]

Polymer abbreviation	Polymer composition[a] (mol%)		No. of PEGMA units per polymer chain[a]	No. of MAPTAC units per polymer chain[a]	M_n[a]	PDI[b]
	MAPTAC	PEGMA				
PMAPTAC	100.0	0.0	0	80	18,000	1.10
BBCP31	31.0	69.0	178	80	104,000	1.37
BBCP16	16.0	84.0	420	80	220,000	1.46

[a]By 1H NMR from, [b]By GPC

Steady-State Fluorescence and Ethidium Bromide Exclusion Assay: Interactions between cationic BBCPs and *ct*DNA were investigated by ethidium bromide (EB) dye exclusion assay. It is known that EB binds to DNA by intercalation into the base pairs, thereby stretching the double helix of DNA that illuminate under fluorescence.[35] DNA intercalated EB dye can be effectively displaced from the DNA double helix by cationic agents such as multivalent cations, surfactants, dendrimers or polymers. As a result of exclusion, the surrounding environment of the EB dye changes from hydrophobic (DNA helix) to hydrophilic (aqueous medium). Therefore, fluorescence intensity of the DNA-EB complex is reduced in presence of cationic agents, suggesting an effective binding between the DNA and the cationic agents. In the present case also, the reduction in the fluorescence intensity on displacement of EB molecules from the DNA double helix by the BBCPs was used to monitor the cationic BBCP-*ct*DNA polyplex formation. Figure 1a-b show the steady state fluorescence intensities of the EB-DNA complex on addition of the two BBCPs. Fluorescence signals of the EB-*ct*DNA complexes gradually decreased with increase in the concentration of the BBCPs in the solution. Reasonably

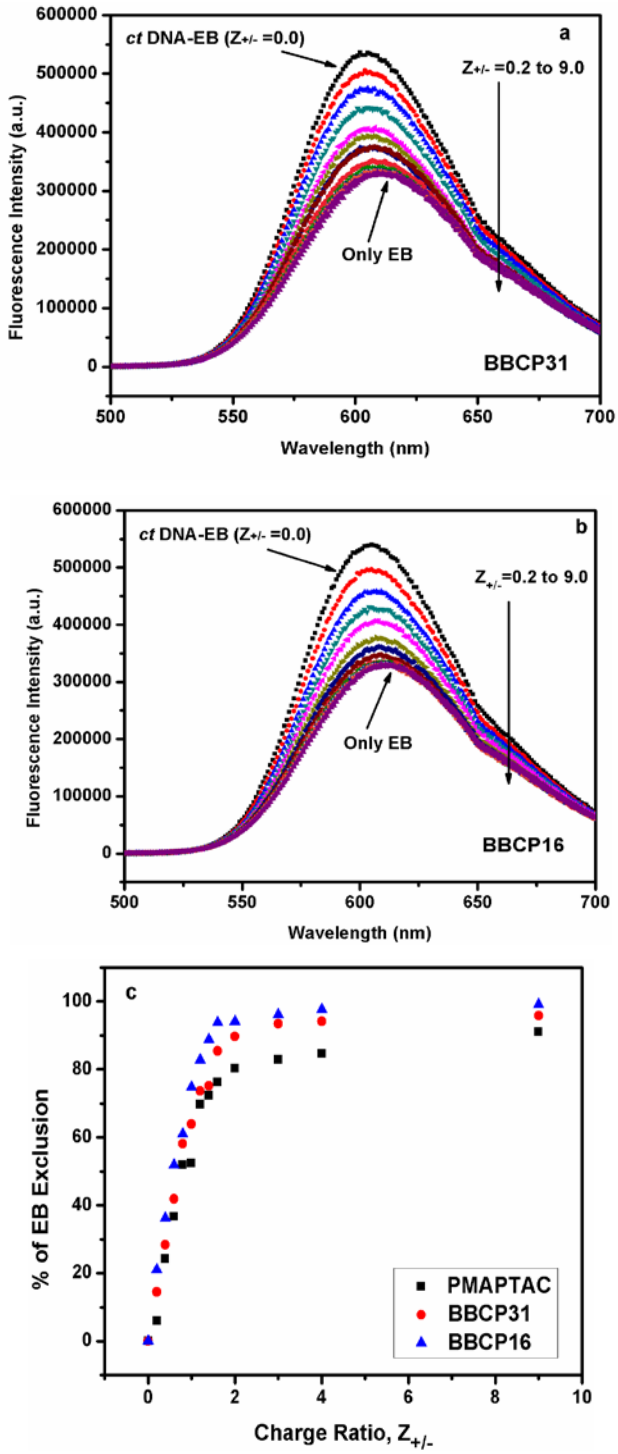

Figure 1: Fluorescence spectra of ethidium bromide (EB) - DNA complex in presence of various amount of (a) BBCP31 (b) BBCP16; traces for fluorescence emission spectra of free EB and EB bound to *ct*DNA are marked by arrows. Percentage of EB exclusion from *ct*DNA - EB complex in presence of various cationic polymers are shown in (c).

high quantities of EB were excluded, suggesting a significantly strong *ct*DNA-BBCP interaction. In Fig 1c, a comparison of the exclusion efficiencies has been shown. It is clearly that BBCP16 displaced the highest amount of EB (99 % at $Z_{+/-}$ = 9) while PMAPTAC displaced the lowest amount of EB (91 %, at $Z_{+/-}$ = 9) in the series, at the same charge ratio. Thus, the relative binding affinities of the cationic BBCPs followed the order: BBCP 16 > BBCP31 > PMAPTAC, which is in accordance with decreasing PEG content in the polymers.

Qualitative comparison between the binding constants of the copolymers with *ct*DNA can also be obtained from the concentration of the cationic polymers required to exclude 50% of EB.[6,36] The following eq. 2 has been used to calculate the apparent binding constants and free energy changes,

$$K_{EB}C_{EB} = K_{PMAPTAC}C_{PMAPTAC\text{-}50\%} = K_{BBCP31}C_{BBCP31\text{-}50\%} = K_{BBCP16}C_{BBCP16\text{-}50\%} \quad \text{- eq. 2}$$

C_{EB} is the concentration of EB dye used in this study (12.5 μM). K_{EB} is the binding affinity of ethidium bromide for *ct*DNA and was taken as 2.8×10^5 M^{-1} at 25 °C from previously reported value.[6] $K_{PMAPTAC}$, K_{BBCP31}, and K_{BBCP16} are the apparent binding constants of PMAPTAC, BBCP31 and BBCP16 respectively with *ct*DNA. $C_{PMAPTAC\text{-}50\%}$, $C_{BBCP31\text{-}50\%}$, and $C_{BBCP16\text{-}50\%}$ are the concentrations (in terms of cationic charge) required to exclude 50% of bound ethidium bromide, for PMAPTAC, BBCP31 and BBCP16 respectively. The values of the apparent binding constants $K_{PMAPTAC}$, K_{BBCP31} and K_{BBCP16} are given below. The apparent binding affinities were of the order of 10^5 M^{-1} (in terms of cationic charge concentration) for the BBCPs studied here, indicating strong binding between the *ct*DNA and BBCPs. The values for the binding constants were 1.8×10^5 M^{-1}, 2.0×10^5 M^{-1} and 2.4×10^5 M^{-1} for PMAPTAC, BBCP31 and BBCP16 respectively. If we compare the apparent binding constant values with the binding

constants of random cationic copolymers as reported by C.K. Nisha et al,[6] we see that these cationic BBCPs can more effectively bind with DNA in comparison to their random counterpart.

We believe that at higher charge ratio, when charge neutralization process was over, the concentration of PEG units around the charge neutralized DNA moiety increased significantly. In this situation, hydrophobic interactions between the PEG residues of the cationic BBCPs and the DNA base pairs became effective The hanging PEG units of the BBCPs additionally took part in the DNA condensation process in a reinforcing manner. Poly(ethylene glycol)s are well known DNA condensing agent at high concentrations, by virtue of their crowding effect around DNA chains.[37-38] At higher charge ratios, where the charge neutralization process was complete, the PEG units helped in condensing the DNA chains further by the crowding effect, resulting in displacement of a major portion of the residual intercalated EB molecules from the DNA helix (Figure 1c). It is also noteworthy that in the case of PEGylated polyplexes the relatively higher value of EB release could also be possibly due to the decreased accessibility of the EtBr to the DNA due to the presence of the PEG moieties. However, in the present study, as the BBCPs were added to the preformed strong EtBr-DNA complex, the release of EB from a DNA-bound state into the aqueous phase is more likely because of the compaction of DNA on complexation with the BBCPs.

Melting of BBCP-DNA Polyplexes: Melting temperatures (T_m) derived from the UV-melting profiles, provide important information about the helix-coil-globule transitions of the DNA polyplexes. This technique has been frequently used for characterization of DNA polyplexes as it can predict the existence as well as the stability of the DNA polyplexes.[6,39] Determination of T_m values of *ct*DNA-BBCP complexes at various charge ratios ($Z_{+/-}$) would indicate the extent to which the compositions of the BBCPs influence the stability of the *ct*DNA. Normally, an

increase in the absorbance (hyperchromic effect) is observed on melting of the DNA, mainly due to disruption of the base stacking in the double-stranded DNA resulting from breakage of the hydrogen bonds.[40] Melting profiles of the BBCP-DNA polyplexes at two different charge ratios ($Z_{+/-}$= 0.50 and 1.0) in 10 mM phosphate buffer are shown in Figure 2. The melting curves showed sigmoidal behavior. A transition was seen around 72 °C in case of the polymer-*ct*DNA mixtures at lower $Z_{+/-}$ values, which corresponded to the melting of slightly compacted *ct*DNA present in the polyplexes. For lower $Z_{+/-}$ values, there could be another melting transition close to, or above 100 °C, for the *ct*DNA present in the more compact polyplexes, which could not be detected in the melting experiments. Initially, after the melting just started, the absorbance values decreased with increasing $Z_{+/-}$. It indicated the reduction in the quantity of free DNA in the solution. Different extents of loss of absorption were observed with increasing temperature, which was highest for PMAPTAC whereas PEGylated cationic blocks showed lesser loss of absorption. Similar observation has been reported earlier for such polyelectrolyte systems.[41,42] At higher $Z_{+/-}$ values, no transition around 72 °C was observed for the copolymers with less PEG or no PEG, indicating that the formed polyplexes are sufficiently strong to prevent DNA melting altogether. Strong electrostatic interactions between the positively charged units of BBCPs and the negatively charged phosphate groups of DNA resulted in a reduction of the electrostatic repulsion between the phosphate groups present in the DNA backbone, thus stabilizing the helical structures of DNA.[43]

Dynamic Light Scattering (DLS) Measurements: DLS technique provides important information regarding the average hydrodynamic size and the size distribution of free *ct*DNA and DNA-cationic BBCP polyplexes. Figure 3 shows the variation of Z-average hydrodynamic

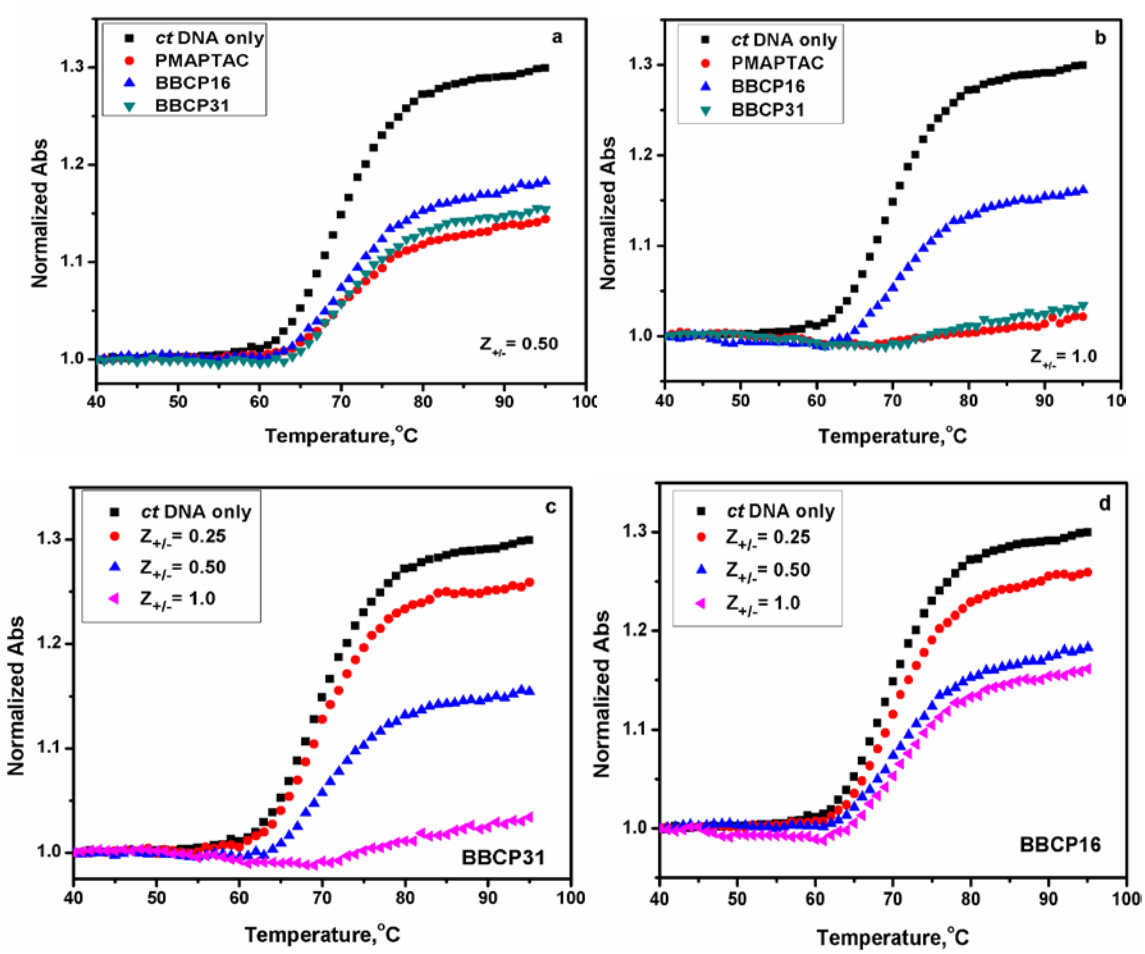

Figure 2. Comparison of UV melting profiles of BBCP bound *ct*DNA complexes at different charge ratios - (a) $Z_{+/-}$ = 0.50, (b) $Z_{+/-}$ =1.0 and (c) BBCP31 (d) BBCP16.

diameter (D_H) of *ct*DNA (solution concentration of DNA is same as used in fluorescence measurement study) in the presence and absence of cationic BBCPs at different $Z_{+/}$. Existence of three different regions in the average size of the DNA-BBCP polyplexes with variation of $Z_{+/-}$ has been found. From figure 3, it is clear that with an increase in the BBCP content, a steady decrease of D_H from ~ 700 nm to ~ 120-130 nm for the *ct*DNA-BBCP mixtures occurred below $Z_{+/-}$ ~ 1.0. Between $Z_{+/-}$ ~ 1.0 to $Z_{+/-}$ ~ 1.8, the D_H remained nearly same. Above $Z_{+/-}$ ~ 2.0, the D_H of the polyplexes increased, first slightly and then drastically, to about 1600-2000 nm in case of the two BBCPs. In this case, the D_H data were obtained directly from instrument's software that

analyzed auto-correlation function by CUMMULANT analysis method. It is known that CUMMULANT analysis method sometimes leads to incomplete/misleading information about sizes and their relative abundances when system is highly polydisperse, like the present case. Hence, the autocorrelation function was further analyzed by CONTIN algorithm and the intensity-weighted DLS histograms for the two BBCP-*ct*DNA systems, at varying $Z_{+/-}$ are shown in Figure 4. Table S1 (ESI) shows the different sizes of the DNA polyplexes at different $Z_{+/-}$ values with the two BBCPs. Initially a monomodal size (~780 nm) distribution was found for the free native *ct*DNA. Gradually, a bimodal size distribution appeared at low to medium values of $Z_{+/-}$, but the size distribution became monomodal once again at higher $Z_{+/-}$. Size distribution profiles as well as the data presented at Table S1 (ESI) clearly indicate that when cationic BBCPs were added to the DNA solutions, two different populations of DNA molecules appeared. This established the fact that two types of DNA-polyplexes with different sizes and different levels of compaction co-existed. The size compaction was found to be maximum at $Z_{+/-}$ ~ 1, above which, the average size of the BBCP polyplexes increased significantly. Results suggested that around $Z_{+/-}$ ~ 1, the flexible DNA chains were compacted in a globular conformation. At higher charge ratios, the globular compact DNA polyplexes interacted amongst themselves leading to the formation of aggregates of larger sizes. From Table S1, it is obvious that BBCP16 led to slightly more compaction of DNA chains compared to BBCP31 at the same $Z_{+/-}$, till ~ $Z_{+/-}$ = 1. This is true for both the DNA-polyplex species present in the mixture. For example, at $Z_{+/-}$ = 0.6, the two polyplexes have Z-average D_H values of 255 nm and 77 nm for BBCP31, whereas for BBCP16 the sizes were 143.4 nm and 39.7 nm. This variation in the size may be explained in terms of PEG content of the BBCPs, as PEG is already known for such kind of DNA condensing ability. In case of BBCP16, the number of hanging PEG units were much

more compared to BBCP31, thus helping to compact *ct*DNA to a larger extent. In our previous work,[13] we have reported similar kind of DNA compaction study by linear cationic block copolymer containing linear PEG units. Size compaction of *ct*DNA also occurred in that case, but not to the extent as the present case, since in the linear cationic blocks copolymers the content of linear PEG units were much less compared to the content of hanging PEG units in the present BBCP. In case of PMAPTAC with no PEG content, compaction of DNA occurred only because of the cationic PMAPTAC unit.

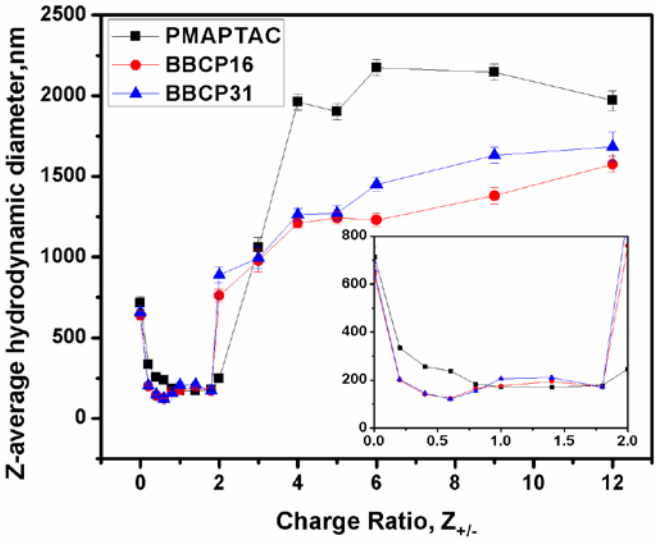

Figure 3: Z-average hydrodynamic diameters of ctDNA-BBCP polyplexes obtained from dynamic light scattering measurements are plotted as a function of $Z_{+/-}$. Here, the data were obtained directly from the instrument's software that analyzes autocorrelation function by CUMMULANT analysis method.

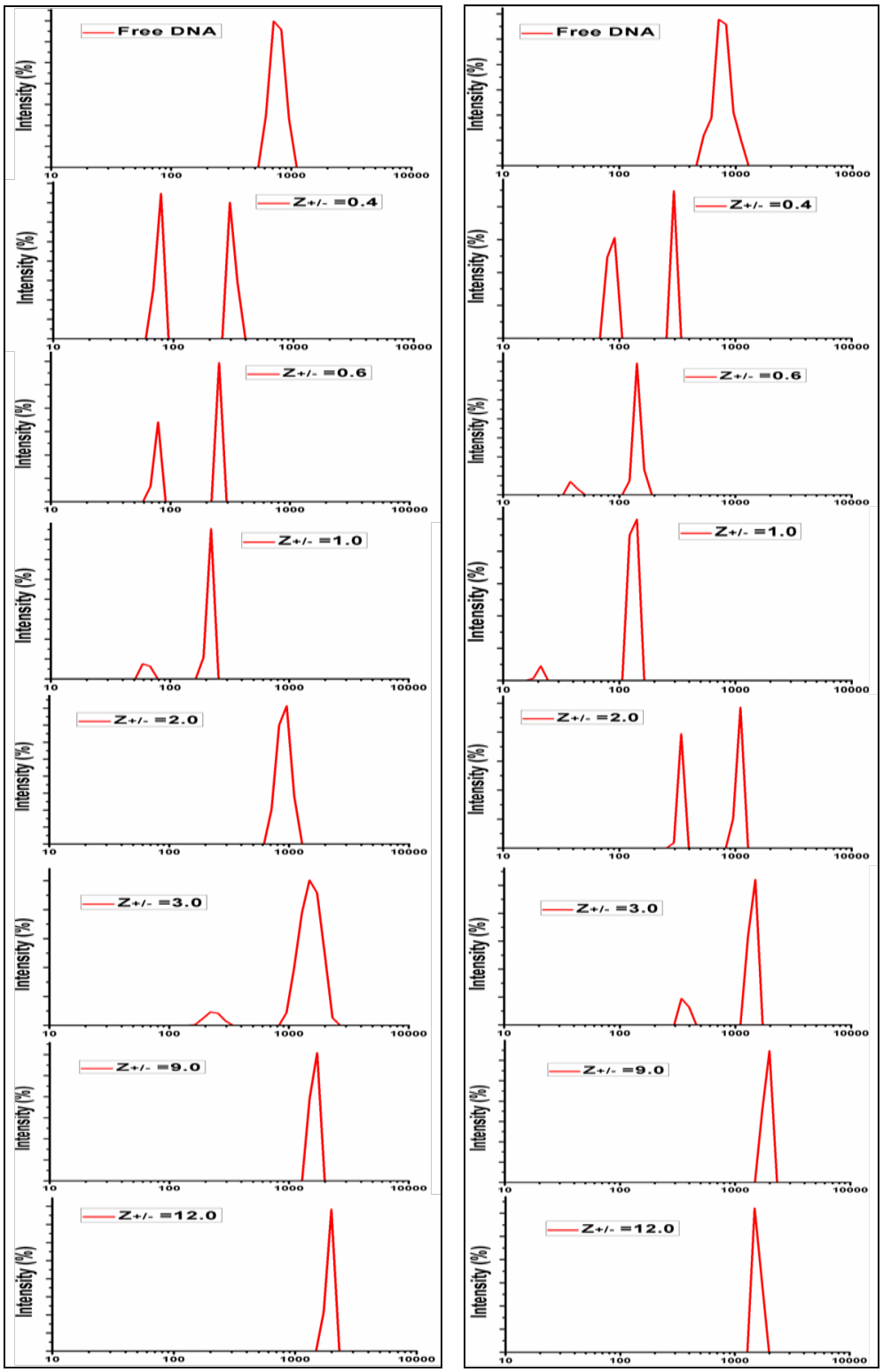

Figure 4. DLS histograms showing the intensity distribution profiles of BBCPs bound *ct*DNA complexes at different charge ratios (x-axis: hydrodynamic diameter, nm; deconvolution of the autocorrelation function were carried out using CONTIN software). Left part (BBCP31), Right part (BBCP16).

Circular Dichroism Measurements: Circular dichroism study revealed the possible conformational changes occurring in native *ct*DNA upon formation of the polyplexes with the cationic BBCPs. Figure 5 shows the CD spectra of native *ct*DNA and BBCP-DNA polyplexes at different charge ratios. Three major peaks at 220 nm (positive), 245 nm (negative) and 275 nm (positive) in the CD spectra are characteristics of free *ct*DNA. This confirmed the double helical structure of *ct*DNA in B conformation.[37] Positive band at 275 nm is due to the base stacking and negative band at 245 nm is due to polynucleotide helicity.[37] None of our BBCPs has any optical activity.

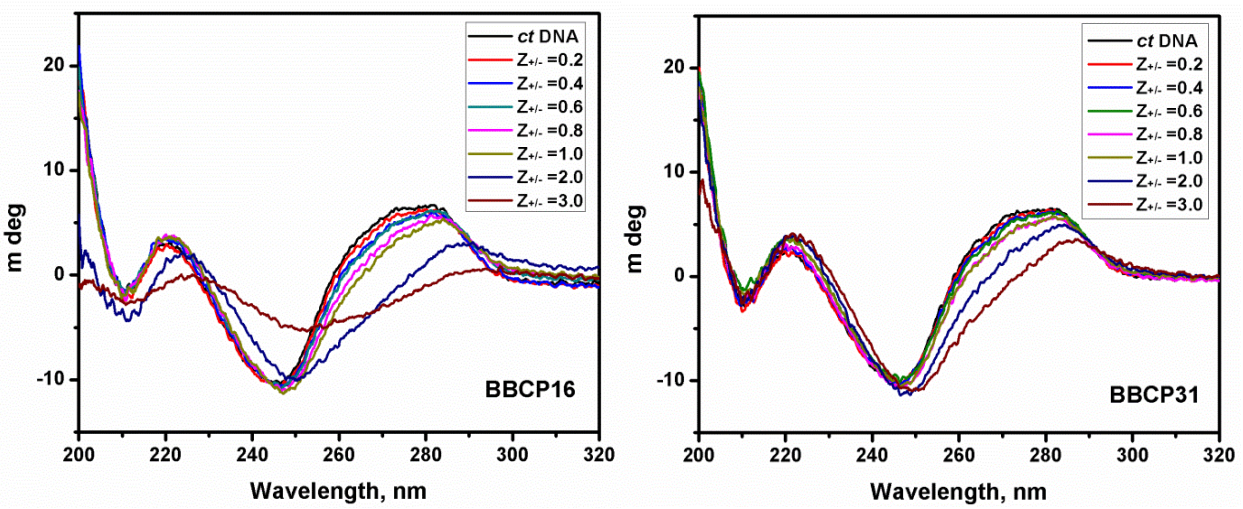

Figure 5: CD spectra of free *ct*DNA and DNA polyplexes at different charge ratios, $Z_{+/-}$.

Upon addition of a cationic polymer, a significant decrease in molar ellipticity of the band at 275 nm was observed, while the negativity of the band at 245 nm increased upto $Z_{+/-}$ =1.0. However, the nature of the spectra remained nearly unchanged, demonstrating that DNA remained in B conformation upon complexation with the BBCPs. From $Z_{+/-}$ >1.0, the spectra were flattened out. The condensation observed here is qualitatively different from the multimolecular ψ-DNA condensation induced by PEG and sodium chloride, [44] the aggregates formed in the present case

at $Z_{+/-}$ >1.0 are not exactly a pure condensed phase of DNA but are the aggregates of DNA-polyelectrolyte polyplexes. Figure 5 clearly shows that BBCP16 with higher PEG content perturbed the DNA structures much more compared to the less PEGylated BBCP31 at the same $Z_{+/-}$ values. The higher numbers of hanging PEG units in BBCP16 actively participate in condensing DNA to a maximum level in the series.

Stopped-Flow Fluorescence Spectroscopic Studies and Kinetic measurements: Any potential polycation gene delivery agent must satisfy two important criteria (i) ability to completely neutralize the charge of the native DNA leading to a more compact state of the polyplexes formed by DNA and polycation, and (ii) dissociation of the DNA-polycation complexes in the cytoplasm of the target cell.[7,45-46] In this connection, the kinetic parameters of the DNA polyplex formation process could provide some vital information. We have used stopped-flow fluorescence technique to monitor the kinetic parameters of the process. In addition to the BBCPs-*ct*DNA charge ratios, the effect of the composition of the cationic bottle-brush block copolymers on the kinetic parameters has been investigated**.**

Figure S1a (ESI) shows a typical fluorescence intensity decay of *ct*DNA-EB complex observed upon binding of BBCP31 to *ct*DNA at $Z_{+/-}$ = 1.0 in 10 mM phosphate buffer solution. The kinetic curves showed multi-exponential decay and were analyzed by fitting them to a sum of exponentials (eq 1). The number of exponentials was increased until no systematic deviation of the residual was found (as shown in Figure S1b (ESI)). Figure 6 shows experimental plots of *ct*DNA-EB fluorescence intensity decay as a function of time at 25 °C for each of the two cationic BBCPs at three different charge ratios ($Z_{+/-}$ = 1.0, 3.0, 9.0). The fluorescence decay curves were fitted to eq. 1**.** The rate constants for the different BBCPs (including PMAPTAC[13])

as a function of $Z_{+/-}$ at constant DNA concentration and temperature are shown in Table S2. Each rate-constant is the average of three independent experiments. These rate constants are relative in nature as the absolute value depends on several factors including the choice of the dye.[28, 34, 47] The values of these rate constants were separated by at least an order of magnitude for all the BBCPs under investigation. The polyplex formation followed a bimolecular mechanistic pathway. We obtained two relative rate constants ($k_1^{'}$ and $k_2^{'}$) for the binding process from the exponential plots which followed the order $k_1^{'} > k_2^{'}$.

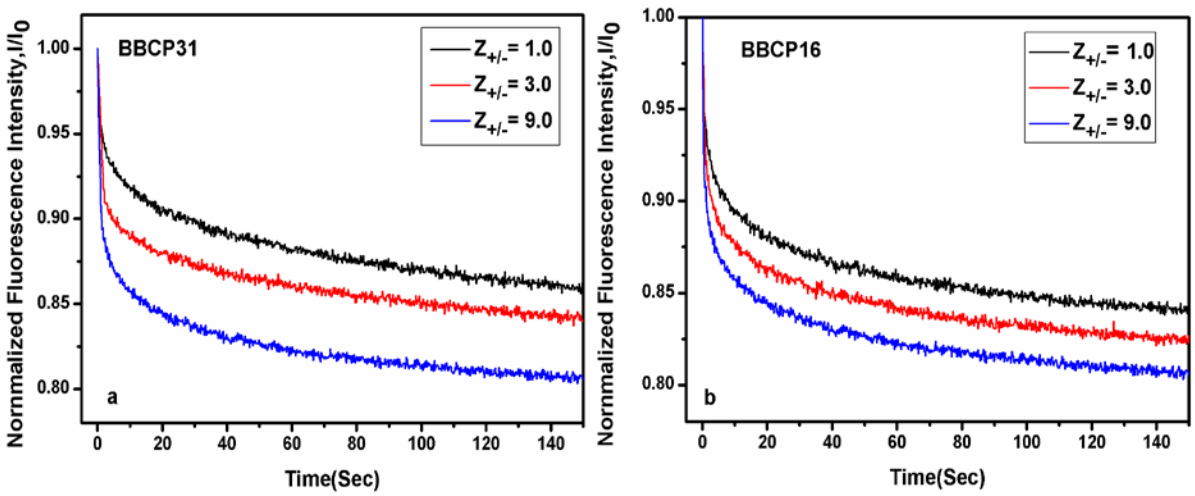

Figure 6: Fluorescence intensity of *ct*DNA-EB complex as a function of time after mixing with BBCPs at different BBCPs to *ct*DNA charge ratio ($Z_{+/-}$= 1.0, 3.0, and 9.0); (a) BBCP31 (b) BBCP16.

All fluorescence emission decay curve fitted into the bi-exponential function, suggesting the involvement of a two-step process in the polyplex formation. In general, the initial step of the complexation was found to be very fast in all the cases, which corresponded to a process driven by electrostatic interactions. Accordingly, the first rate constant $k_1^{'}$ increased with increase in $Z_{+/-}$. The second step was slower compared to the first one, corresponding to the compaction of *ct*DNA with a simultaneous internal rearrangement of the *ct*DNA-BBCP complex after the initial

fast binding.[28, 34, 47] As shown in Figure 7, The $k_2^{'}$ values were also found to increase with increase in $Z_{+/-}$, although the increase was less compared to $k_1^{'}$. This is expected as the second step involved the compaction of large DNA molecule. At higher $Z_{+/-}$, the presence of higher amount of cationic BBCPs in the negatively charged DNA solution facilitated a faster interaction, leading to a faster binding between the two. The second rate constant $k_2^{'}$ also followed a similar trend but the increment was lesser as compared to the $k_1^{'}$ values. Actually, the second step mainly corresponded to DNA condensation process where the electrostatic interaction was no more the lone determining factor. Internal rearrangements within the DNA secondary structure occurred in this step, which led to compaction of the DNA chains. This was indeed a slower process compared to the first one.

Polyplex formation between DNA and the cationic polymers is indeed a very complex procedure. Studies related to the kinetics of such polyplex formation process are very limited in literature. A very fast nature of the complexation process makes it rather difficult to study by conventional mixing methods.[48] We have monitored this type of fast kinetic process previously in *ct*DNA-PAMAM dendrimer[34] and *ct*DNA-cationic linear block copolymer (BCP) system[13] by stopped-flow fluorescence method. Although, the values of the rate constants obtained by this method are relative in nature, it can still provide vital information regarding the kinetic pathway.

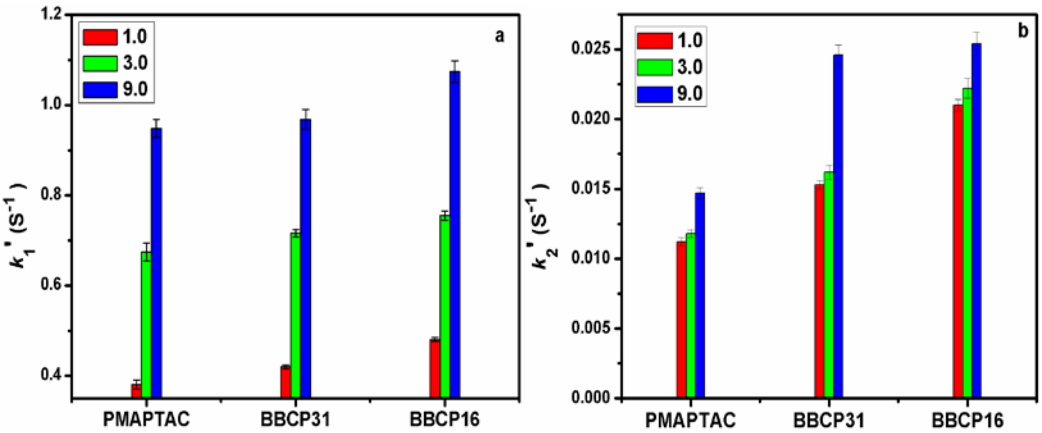

Figure 7: Comparison of rate constants in case of different BBCPs at different charge ratios (a) $k_1^{'}$, (b) $k_2^{'}$.

The binding kinetic studies showed fluorescence intensity decay of EB-bound *ct*DNA in presence of different BBCPs at different charge ratios (Figure 6). Consideration of bi-exponential decay (two-step mechanism) was good enough to explain our present system. For determining the effect of the composition of the cationic BBCPs on the two rate constants, we looked again into the structures of the BBCPs under study. PMAPTAC, being a cationic homopolymer with no PEG content, was expected to interact with *ct*DNA in a way similar to any other cationic polyelectrolyte system. Between the two cationic BBCPs under investigation, BBCP16, with the highest PEG content, showed the maximum value for both the rate constants. This may be explained by the fact that at a fixed $Z_{+/-}$, hydrophobic interactions between the hanging PEG chains and the DNA base pairs came into play whereas, in case of PMAPTAC system, this kind of effect was absent. Increase in the value of $k_1^{'}$ from PMAPTAC to the BBCPs, suggested synergistic operative mode of crowding effect of the hanging PEG block units in addition to the electrostatic binding process, owing to the presence of large excess of PEG chains in the surroundings of the DNA chains in aqueous medium. Similarly, $k_2^{'}$ was also found to increase from PMAPTAC to the BBCPs, which could be explained on the basis of PEG

content in the polymer chains. Presence of higher percentage of PEG in the cationic BBCP16 or BBCP31 promoted higher extent of DNA condensation (as supported by DLS data) as compared to PMAPTAC with no PEG. This may be attributed to effective hydrophobic interactions between polymer and DNA chains at close proximity in the condensed state of the DNA. A comparison of the values of the two rate constants of the BBCPs-*ct*DNA complexation process with our previous results with linear cationic BCPs-*ct*DNA complexation process[13] revealed a significant difference in the values of $k_1^{'}$, although the values of $k_2^{'}$ were almost similar. In the present case with BBCPs, the values of first rate constant $k_1^{'}$ at same charge ratio were found to be comparatively higher compared to PMAPTAC or previously reported studies with linear BCPs.[13] This might be due to crowding of large excess of hanging PEG units in the close surroundings of the DNA chains. In the present case, the first step involves strong electrostatic interaction as well as crowding effect of large number of hanging PEG units acting in tandem. This effect is not so much prominent in the first kinetic step of DNA binding with linear cationic block copolymers[13] reported previously, as the PEG content is relatively less in those cases compared to the present BBCPs.

CONCLUSIONS:

All the cationic BBCPs under investigation were capable of binding effectively with negatively charged calf-thymus DNA through electrostatic interactions. BBCP with a higher PEG content showed slightly more binding efficiency towards DNA. Synergistic hydrophobic interactions between the hanging PEG units of the cationic BBCPs and the *ct*DNA base pairs contributed significantly towards the overall binding process, in addition to the normal electrostatic interactions present in the system. In addition, a study of the binding kinetics by stopped-flow technique revealed that the BBCPs with higher PEG content could bind faster with

the DNA compared to PMAPTAC homopolymer, where PEG content was nil. BBCPs with higher PEG content led to compaction of the DNA chains to a much greater extent as compared to those with lower PEG content. Crowding effect of hanging PEG units plays a vital role in compaction of DNA chains in addition to the normal electrostatic compaction.

ACKNOWLEDGEMENT

Financial support from SRIC, Indian Institute of Technology Kharagpur (project codes ADA, NPA with institute approval numbers - IIT/SRIC/CHY/ADA/2014-15/18 and IIT/SRIC/CHY/NPA/2014-15/81 respectively) is acknowledged. The authors acknowledge Prof. N. Sarkar for providing some laboratory facilities. D. Dey and C. Maiti acknowledges UGC, New Delhi for Senior Research Fellowships. The authors are thankful to one of the reviewers for useful and constructive suggestions.

ELECTRONIC SUPPORTING INFORMATION

Stopped-flow decay fitting with residuals, size of different polyplexes with their relative abundances, and numerical values of two rate constants are provided in the supporting information.

REFERENCES:

1. T. Niidome and L. Huang, Gene Therapy Progress and Prospects: Nonviral Vectors, *Gene Therapy*, 2002, **9**, 1647-1652.
2. W. F. Anderson, Human Gene Therapy, *Science*, 1992, **256**, 808-813.
3. G. Zuber, E. Dauty, M. Nothisen, P. Belguise and J. P. Behr, Towards synthetic Viruses. *Adv. Drug Delivery Rev.*, 2001, **52**, 245-253.

4. K. Kataoka, A. Harada and Y. Nagasaki, Block Copolymer Micelles for Drug Delivery: Design, Characterization and Biological Significance, *Adv. Drug Delivery Rev*., 2001, **47**, 113-131.

5. Y. Kakizawa and K. Kataoka, Block Copolymer Micelles for Delivery of Gene and Related Compounds, *Adv. Drug Delivery Rev*., 2002, **54**, 203-222.

6. C. K. Nisha, S. V. Manorama, M. Ganguli, S. Maiti and J. N. Kizhakkedathu, Complexes of Poly(ethylene glycol)-Based Cationic Random Copolymer and Calf Thymus DNA: A Complete Biophysical Characterization, *Langmuir*, 2004, **20**, 2386-2396.

7. R. S. Dias and B. Lindman, DNA Interactions with Polymers and Surfactants, Wiley and Sons: Hoboken, NJ, 2008.

8. S. Marchetti, G. Onori and C. Cametti, DNA Condensation Induced by Cationic Surfactant: A Viscosimetry and Dynamic Light Scattering Study, *J. Phys. Chem. B*, 2005, **109**, 3676−3680.

9. S. D. Smedt, J. Demeester and W. E. Hennink, Cationic Polymer Based Gene Delivery Systems, *Pharm. Res.*, 2000, **17**, 113-126.

10. T. K. Bronich, H. K Ngueyen, A. Eisenberg and A. V. Kabanov, Recognition of DNA Topology in Reactions Between Plasmid DNA and Cationic Copolymers, *J. Am. Chem. Soc.*, 2000, **122**, 8339-8343.

11. W. C. Tseng and C. M. Jong, Improved Stability of Polycationic Vector by Dextran-Grafted Branched Polyethylenimine, *Biomacromolecules*, 2003, **4**, 1277-1284.

12. W. A. Braunecker and K. Matyjaszewski, Controlled/Living Radical Polymerization: Features, Developments, and Perspectives, *Prog. Polym. Sci.*, 2007, **32**, 93-146.

13. D. Dey, S. Kumar, R. Banerjee, S. Maiti and D. Dhara, Polyplex Formation between PEGylated Linear Cationic Block Copolymers and DNA: Equilibrium and Kinetic Studies, *J. Phys. Chem. B.*, 2014, **118**, 7012-7025.

14. G. Moad, E. Rizzardo and S. H. Thang, Reversible Addition Fragmentation Chain Transfer (RAFT) Polymerization, *Mater Matter*. , 2010, **5**, 2-4.

15. J. Chiefari, Y. K. Chong, F. Ercole, J. Krstina., J. Jeffery and T. P. T. Le, Living Free Radical Polymerization by Reversible Addition-Fragmentation Chain Transfer The RAFT Process, *Macromolecules*, 1998, **31**, 5559-5562.

16. R. Banerjee, S. Gupta, D. Dey, S. Maiti and D. Dhara, Synthesis of PEG Containing Cationic Block Copolymers and Their Interaction with Human Serum Albumin, *Reactive and Functional Polymers*, 2014, **74**, 81-89.

17. R. S. Dias, J. Innerlohinger, O, Glatter, M. G. Miguel, and B. Lindman, Coil-Globule Transition of DNA Molecules Induced by Cationic Surfactants: A Dynamic Light Scattering Study , *J. Phys. Chem. B*, 2005, **109**, 10458-10463.

18. M. Rosa, R. Dias, M. G. Miguel, and B. Lindman, DNA-Cationic Surfactant Interactions Are Different for Double and Single-Stranded DNA, *Biomacromolecules*, 2005, **6**, 2164-2171.

19. M. Cardenas, T. Nylander, R. K. Thomas, and B. Lindman, DNA Compaction onto Hydrophobic Surfaces by Different Cationic Surfactants, *Langmuir*, 2005, **21**, 6495-6502.

20. R. S. Dias, L. M. Magno, A. J. M. Valente, D. Das, P. K. Das, S. Maiti, M. G. Miguel, and B. Lindman, Interaction between DNA and Cationic Surfactants: Effect of DNA Conformation and Surfactant Headgroup, *J. Phys. Chem., B* 2008, **112**, 14446–14452.

21. M. F. V. Pinto, M. C. Moran, M. G. Miguel, B. Lindman, A. S. Jurado, and A. C. C. Pais, Controlling the Morphology in DNA Condensation and Precipitation, *Biomacromolecules*, 2009, **6**, 1319-1323.

22. S. Marchetti, G. Onori and C. Cametti, Calorimetric and Dynamic Light-Scattering Investigation of Cationic Surfactant-DNA Complexes, *J. Phys. Chem. B*, 2006, **110**, 24761−24765.

23. T. Bronich, A. V. Kabanov, and L. A. Marky, A Thermodynamic Characterization of the Interaction of a Cationic Copolymer with DNA, *J. Phys. Chem. B*, 2001, **105**, 6042-6050.

24. Z. Yang, G. Sahay, S. Sriadibhatla, and A. V. Kabanov, Amphiphilic Block Copolymers Enhance Cellular Uptake and Nuclear Entry of Polyplex-Delivered DNA, *Bioconjugate Chem.*, 2008, **19**, 1987–1994.

25. T. K. Bronich, H. K. Nguyen, A. Eisenberg and A. V. Kabanov, Recognition of DNA Topology in Reactions between Plasmid DNA and Cationic Copolymers, *J. Am. Chem. Soc.*, 2000, **122**, 8339-8343.

26. V. G. Sergeyev, O. A. Novoskoltseva, O. A. Pyshkina, A. A. Zinchenko, V. B. Rogacheva, A. B. Zezin, K. Yoshikawa, and V. A. Kabanov, Secondary Structure of DNA Is Recognized by Slightly Cross-Linked Cationic Hydrogel, *J. Am. Chem. Soc.*, 2002, **124**, 11324-11333.

27. V. Kabanov, I. V. Astafieva, I. V. Maksimova, E. M. Lukanidin ,G. P. Georgiev, V. A. Kabanov, Efficient Transformation of Mammalian Cells Using DNA Interpolyelectrolyte Complexes with Carbon Chain Polycations, *Bioconjugate Chem.*, 1993, **4**, 448-454.

28. P. C. A. Barreleiro and B. Lindman, The Kinetics of DNA-Cationic Vesicle Complex Formation, *J. Phys. Chem. B*, 2003, **107**, 6208-6213.

29. C. S. Braun, M. T. Fisher, D. A. Tomalia, G. S. Koe, J. G. Koe and C. R. A. Middaugh, Stopped-Flow Kinetic Study of The assembly of Nonviral Gene Delivery Complexes, *Biophysical Journal*, 2005, **88**, 4146-4158.

30. E. Grueso, E. Roldan and F. Sanchez, Kinetic Study of The Cetyl trimethylammonium/DNA Interaction, *J. Phys. Chem. B*, 2009, **113**, 8319-8323.

31. R.Y. Wang, X. Gao and Y.T. Lu, A Surfactant Enhanced Stopped-Flow Kinetic Fluorimetric Method for The Determination of Trace DNA, *.Anal. Chim. Acta*, 2005, **538**,151-158.

32. R.Y. Wang, X. Gao and Y.T. Lu, A Kinetic Spectrophotometric Method for Determination of Nitrile by Stopped-Flow Technique, *Anal. Sci.*, 2006, **2**, 299-304.

33. B. Tonomura, H. Nakatani, M. Ohnishi, J. Yamaguchiito and K. Hiromi, Test Reactions for a Stopped-flow Apparatus - Reduction of 2, 6-dichlorophenolindophenol and Potassium ferricyanide by L-Ascorbic acid, *Analytical Biochemistry*, 1978, **84**, 370-383.

34. D. Dey, S. Kumar, S. Maiti and D. Dhara, Stopped-Flow Kinetic Studies of Poly(amidoamine) Dendrimers-Calf Thymus DNA to Form Dendriplexes, *J. Phys. Chem. B*, 2013, **117**, 13767-13774.

35. W. Chen, N. J. Turro and D. A. Tomalia, Using Ethidium Bromide To Probe the Interactions between DNA and Dendrimers, *Langmuir*, 2000, **16**, 15-19.

36. A. R. Morgan, J. S. Lee, D. E. Pulleyblank, N. L. Murray and D. H. Evans, Review: Ethidium Fluorescence Assays. Part 1. Physicochemical studies, *Nucleic Acids Research*, 1979, **7**, 547-569.

37. E. Froehlich, J. S. Mandeville, D. Arnold, L. Kreplak and H. A. Tajmir-Riahi, PEG and mPEG-Anthracene Induce DNA Condensation and Particle Formation, *J. Phys. Chem. B*, 2011, **115**, 9873–9879.

38. H. Petersen, P. M. Fechner, A. L. Martin, K. Kunath, S. Stolnik, C. J. Roberts, D. Fischer, M. C. Davies and T. Kissel, Polyethylenimine-*graft*-Poly(ethylene glycol) Copolymers: Influence of Copolymer Block Structure on DNA Complexation and Biological Activities as Gene Delivery System, *Bioconjugate Chem.*, 2002, **13**, 845-854.

39. A. Schallon, C. V. Synatschke, D. V. Pergushov, V. Jerome, A. H. E. Muller and R. Freitag, DNA Melting Temperature Assay for Assessing the Stability of DNA Polyplexes Intended for Nonviral Gene Delivery, *Langmuir* , 2011, **27**, 12042–12051.

40. K. J. Breslauer, Extracting Thermodynamic Data from Equilibrium Melting Curves for Oligonucleotide Order-Disorder Transitions, *Methods Enzymol*., 1995, **259**, 221-242.

41. S. Katayose and K. Kataoka, Water-Soluble Polyion Complex Associates of DNA and Poly(ethylene glycol)-Poly(L-lysine) Block Copolymer, *Bioconjugate Chem*., 1997, **8**, 702-707.

42. A. Maruyama, H. Watanabe, A. Ferdous, M. Katoh, T. Ishihara and T. Akaike, Characterization of Interpolyelectrolyte Complexes between Double-Stranded DNA and Polylysine Comb-Type Copolymers Having Hydrophilic Side Chains, *Bioconjugate Chem.* 1998, **9**, 292-299.

43. B. Wolf and S. Hanlon, Structural Transitions of Deoxyribonucleic Acid in Aqueous Electrolyte Solutions. II. The Role of Hydration, *Biochemistry*, 1975, **14**, 1661-1670.

44. J. E. B. Ramos, R. D. Vries, and J. R. Neto, DNA ψ-Condensation and Reentrant Decondensation: Effect of the PEG Degree of Polymerization, *J. Phys. Chem. B*, 2005, **109**, 23661-23665.

45. C. T. D. Ilarduya, Y. Sun and N. Düzgüneş, Gene Delivery by Lipoplexes and Polyplexes, *European Journal of Pharmaceutical Sciences*, 2010, **40**, 159–170.

46. W. T. Godbey and A. G. Mikos, Recent Progress in Gene Delivery Using Non-viral Transfer Complexes, *Journal of Controlled Release*, 2001, **72**, 115–125.

47. D. Santhiya, R. S. Dias, S. Dutta, P. K. Das, M. G. Miguel, B. Lindman and S. Maiti, Kinetic Studies of Amino Acid-Based Surfactant Binding to DNA, *J. Phys. Chem. B*, 2012, **116**, 5831−5837.

48. K. B. Lim and H. L. Pardue, Error-Compensating Kinetic Method for Enzymatic Determinations of DNAs, *Clin. Chem.*, 1993, **39**, 1850-1856.